UNLV | University Libraries
University of Nevada, Las Vegas

Publications (YM) | Yucca Mountain

9-22-2003

Thermal transport eveluations related to waste package design -- model evaluations -- task 19

Roald Akberov
University of Nevada, Las Vegas

Follow this and additional works at: https://digitalscholarship.unlv.edu/yucca_mtn_pubs

 Part of the Mechanical Engineering Commons, and the Software Engineering Commons

Repository Citation

Akberov, R. (2003). Thermal transport eveluations related to waste package design -- model evaluations -- task 19.
Available at: https://digitalscholarship.unlv.edu/yucca_mtn_pubs/55

This Article is protected by copyright and/or related rights. It has been brought to you by Digital Scholarship@UNLV with permission from the rights-holder(s). You are free to use this Article in any way that is permitted by the copyright and related rights legislation that applies to your use. For other uses you need to obtain permission from the rights-holder(s) directly, unless additional rights are indicated by a Creative Commons license in the record and/or on the work itself.

This Article has been accepted for inclusion in Publications (YM) by an authorized administrator of Digital Scholarship@UNLV. For more information, please contact digitalscholarship@unlv.edu.

THERMAL TRANSPORT EVALUATIONS RELATED TO WASTE PACKAGE DESIGN – MODEL EVALUATIONS - TASK 19 -

FINAL REPORT

Nevada Center for Advanced Computational Methods
University of Nevada, Las Vegas
Las Vegas, Nevada

Cooperative Agreement: DE.FC28-98NV12081

September 22, 2003

Originators:

[redacted]
Roald Akberov — 9/22/03 — **Date**

Approvals:

[redacted]
Principal Investigator,
Darrell W. Pepper — 9/22/03 — **Date**

[redacted]
Technical Review,
Hsuan-Tsung Sean Hsieh — 9/22/03 — **Date**

TABLE OF CONTENTS

TABLE OF FIGURES

1 Purpose

The purpose of the "Thermal Transport Evaluations Related to Waste Package Design" Task # 19 of Cooperative Agreement Number DE-FC28-98NV12081 was to develop a new CFDHT model for heat transfer and fluid flow in the potential rsepository at the Yucca Mountain, Nevada and to study the effects of forced convection during the pre-closure period and natural convection during the post-closure period. The analysis was performed for the drift dimensions shown in Figure 4-1 below. The intended use of the model is to estimate the velocity and temperature distribution as well as the highest temperature in the drift during the pre-closure and post-closure periods. The validation of the model is documented in section 6 of this report. The analysis was performed using both STAR-CD v. 3.150 and CFDHT v. 1.0, which are qualified software. The final result is the maximum temperature value in the drift during the pre-closure and post-closure period and the velocity and temperature distribution around the canisters.

2 Quality Assurance

The modeling was performed in accordance with the UCCSN QA program and specifically Quality Assurance Procedures:

QAP 3.0 "Scientific Investigation Control"
QAP 3.1 "Control of Electronic Data"
QAP 3.2 "Software Management"
QAP 3.3 "Analysis and Models"

The portions of the Scientific Notebook, UCCSN-UNLV-023 Volume 2 "Thermal Transport Evaluations Related to Waste Package Design…" pertaining to this report were technically reviewed.

3 Computer Software and Model Usage

The computer software that was used for the simulation of Yucca Mountain drift flow Task 19 was STAR-CD v. 3.150 along with CFDHT v. 1.0. The STAR-CD software is installed on a SGI ONYX 3800 Super Computer running on IRIX 6.5 operating system, located at National Supercomputing Center for Energy and the Environment (NSCEE), at the University of Nevada, Las Vegas (UNLV). The software Tracking Number is UCCSN-002. STAR-CD v. 3.150 is qualified software and used only within the range of validation in accordance with QAP-3.2. The output from STAR-CD will be considered qualified. The CFDHT software is installed on a PC at Nevada Center for Advanced Computational Methods (NCACM), UNLV having the Windows 2000 operating system. The software Tracking Number is UCCSN-001. CFDHT v. 1.0 is qualified software and used only within the range of validation in accordance with QAP-3.2. Results from CFDHT v.1.0 will be designated as qualified. The Tecplot software v. 9.2-0-3 was used for data visualization. No macros or routines were used in Tecplot. All the data files obtained in the Tecplot format were verified manually using a hand calculator as required by UCCSN QAP-3.2. The validation of the model is provided in section 6 of this report, Models. No unqualified software or unqualified data are used.

4 Inputs

The data identification number (DID) for the inputs and outputs supporting this analysis in all sections of this report except for section 6.3 is 019RA.001. All the tables and figures in section 6.3 are taken from Software Definition Report for STAR-CD v.3.150 UCCSN-SDR-002, Software Implementation Report for STAR-CD v.3.150 UCCSN-SIR-002, Software

Definition Report for CFDHT v.1.0 UCCSN-SDR-001, Software Implementation Report for CFDHT v.1.0 UCCSN-SIR-001.

4.1 Data and Parameters

Several sets of inputs were used in the modeling. The inputs are grouped into three categories: Dimensions, Boundary Conditions and Physical Properties. Initial conditions are not considered since the developed model is a steady-state process model. The categories are explained below.

4.1.1 Dimensions

The emplacement area at the Yucca Mountain site was approximated by a rectangular domain of 1060×2550 m [1,2]. The emplacement drifts run along the shorter length of the area. The canisters, all equalized to be 5 m in length and 1.2 m in diameter, were laid down on the floor of the drift in cradles as shown in Figure 4-1.

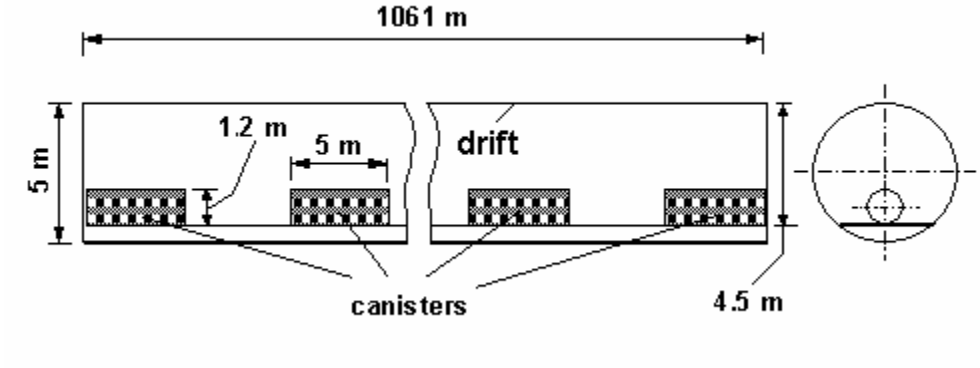

Figure 4-1. Dimensions of the drift and the canister

The number of canisters considered in the simulations was 67, so the spacing between canisters, i.e. the distance between any two canisters can be computed. Only one of the drifts was taken for the analyses.

The 3-d mesh used by STAR-CD for the forced convection calculations for the pre-closure period included only a part of the domain with 46 canisters

instead of 67 for modeling the sequence of canisters in the drift. The mesh is made up of 216,476 tri-linear hexahedral finite elements (usually called “bricks”) with the number of mesh nodes equal to 239,167. A portion of the mesh for the inlet part of the drift is shown in Fig. 4-2.

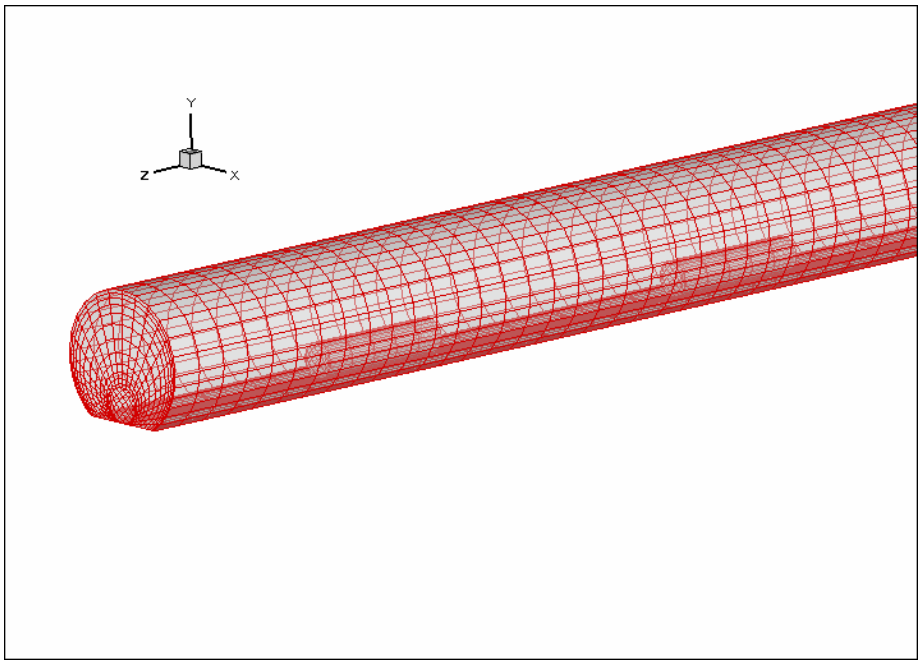

Figure 4-2. 3-D mesh for STAR-CD calculations (019RA.001)

The 3-D mesh used by STAR-CD for the natural convection calculations for the pre-closure period included only a part of the domain with 3 canisters instead of 67 for modeling the sequence of canisters in the drift. The mesh is made up of 11,052 tri-linear hexahedral finite elements with the number of mesh nodes equal to 12,575. The mesh is similar to the mesh shown in Figure 4-2, and therefore it will not be repeated here.

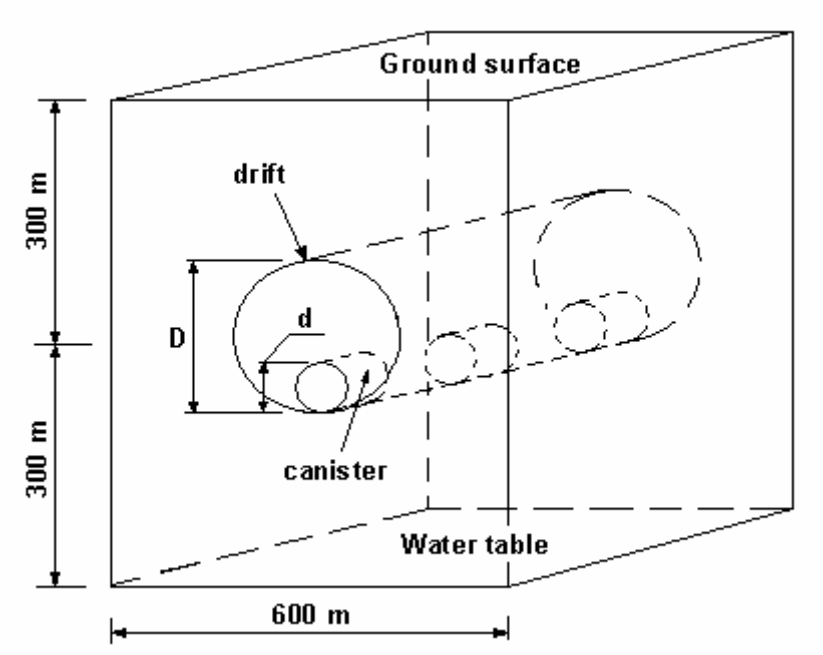

Figure 4-3. Location of the drift at Yucca Mountain

To provide temperature boundary conditions on the drift wall for the STAR-CD natural convection calculations for the post-closure period, the CFDHT v.1.0 software was used to calculate heat conduction through the mountain rock. A similar approach was used by Moujaes [3]. The dimensions given in Figure 4-3 were used in the numerical calculations. In the figure, d=1.2 m is the diameter of the canister, and D=5.0 m is the diameter of the drift. The two distances in the figure denoted as 300 m are the distance from the drift center to the ground surface and the distance from the drift center to the water table. For the heat conduction calculations, the canisters were not considered, only the drift.

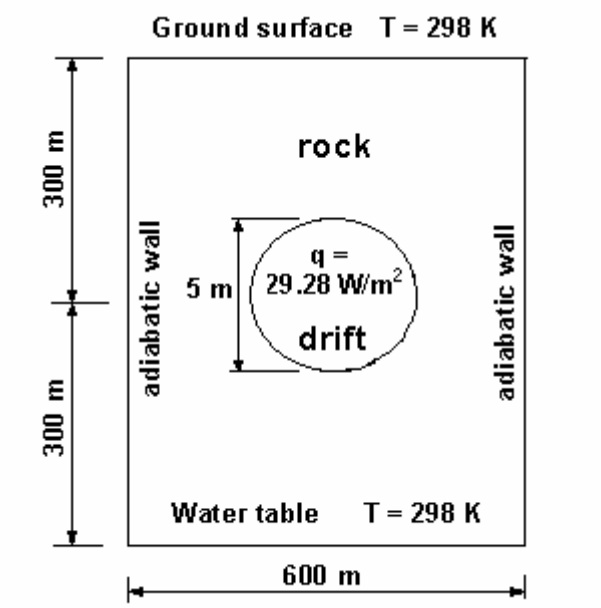

Figure 4-4. Cross section of the view given in Figure 4-3

The CFDHT v.1.0 software performs analyses using the finite element techniques with quadrilateral elements. The diameter of the drift D=5.0 m is relatively small in comparison with the width and height of the two-dimensional cross section of the view in Figure 4-3, which is 600 m. Therefore, the drift for simulations will be approximated as a square of the side length D=5.0 m as shown in Figure 4-5.

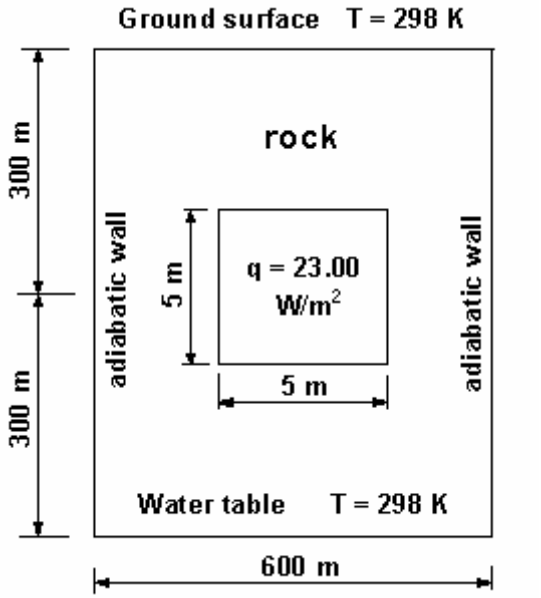

Figure 4-5. Modified cross section of the view given in Figure 4-3

The 2-D mesh used by CFDHT v.1.0 for the heat conduction problem for the post-closure period is made up of 2,401 bi-linear quadrilateral finite elements with the number of mesh nodes equal to 2,500. The mesh is shown in Figure 4-6 below:

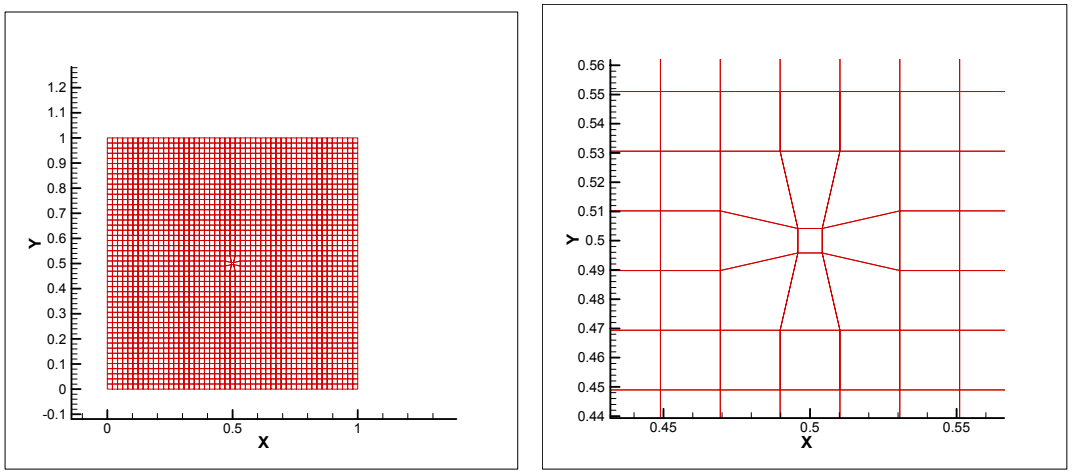

Figure 4-6. The computational mesh 50×50 (on the left - the whole mesh, on the right - zoomed central part). The finite element in the middle is an approximation for the drift.
(019RA.001)

The width and height of the domain in Figure 4-6 are equal to 1.0, because they are nondimensionalized dimensions.

4.1.2 Boundary Conditions

All the calculations performed using both STAR-CD v.3.150 and CFDHT v.1.0 were performed for steady-state conditions.

For the *forced convection* calculations performed by STAR-CD v.3.150, the boundary conditions are given in Figure 4-7 below.

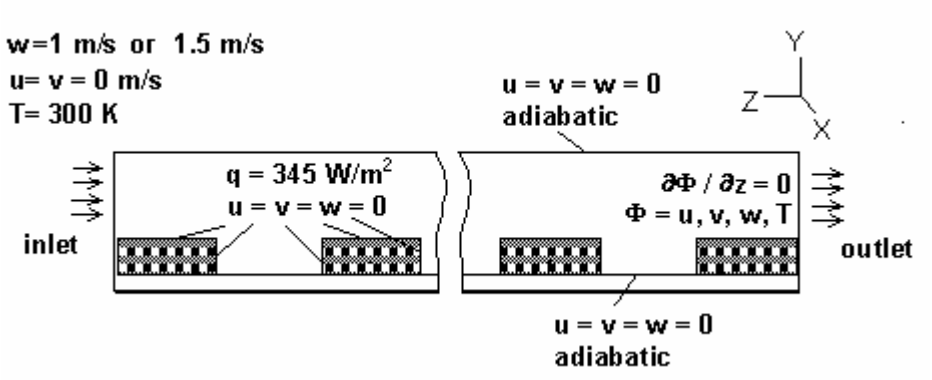

Figure 4-7. Boundary conditions for the forced convection calculations using STAR-CD for the pre-closure period

In the figure, q is the heat flux from the canister; u, v, w are components of the velocity vector defined along X, Y, Z coordinate axes.

The various boundary conditions for the forced convection calculations are:

1. The drift wall and the bottom floor on which canisters are laid are taken as adiabatic wall boundary condition. Non-slip boundary condition for velocities is assumed.
2. On the canisters surface constant heat flux of 345.2 W/m^2 is applied. Non-slip boundary condition for velocities is assumed.
3. Velocity at the inlet is uniform with a magnitude of 1 m/s and 1.5 m/s.
4. At the outlet pressure outlet boundary condition is chosen.

The value of the heat flux of 345.2 W/m^2 is found based on the following.

Each canister in the drift has thermal loading equal to 7,284W. The area of one canister

$$A_{canister} = 3.14159 \times 1.2 \times 5.0 + 2 \times 3.14159 \times 0.6^2 = 18.85 + 2.26 = 21.11 m^2$$

Thus,

$$q_{can} = 7{,}284/21.11 = 345.2\ W/m^2$$

For the *natural convection* calculations performed by STAR-CD v.3.150, the boundary conditions are given in Figure 4-8 below.

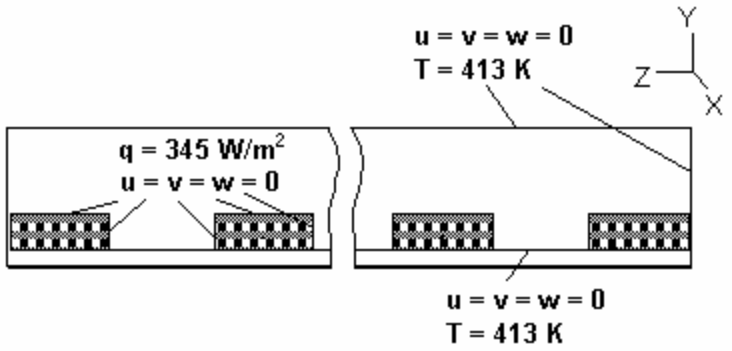

Figure 4-8. Boundary conditions for the natural convection calculations using STAR-CD for the post-closure period

In the figure, q is the heat flux from the canister; u, v, w are components of the velocity vector defined along X, Y, Z coordinate axes.

The various boundary conditions for the natural convection calculations are:

1. The drift wall and the bottom floor on which canisters are laid are taken as isothermal wall boundary condition with the temperature provided with the CFDHT calculations of heat conduction through the mountain rock, i.e. T_{wall}=413*K*. Non-slip boundary condition for velocities is assumed.
2. On the canisters surface constant heat flux of 345.2 W/m^2 is applied. Non-slip boundary condition for velocities is assumed.

For the *heat conduction* calculations performed by CFDHT v.1.0, the boundary conditions are given in Figure 4-9 below.

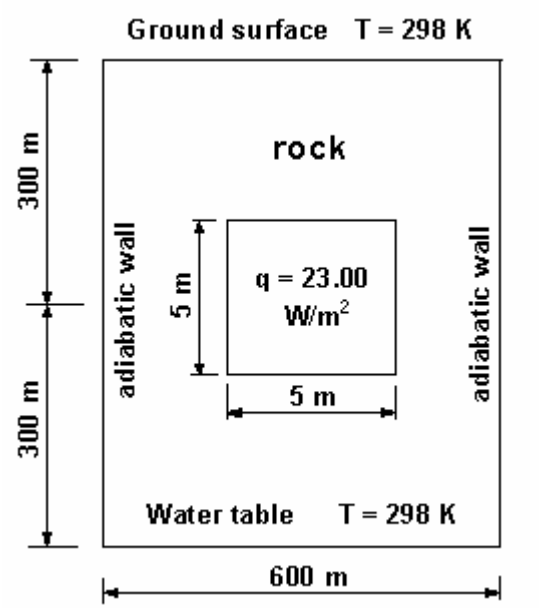

Figure 4-9. Boundary conditions for the heat conduction through rock calculations using CFDHT v.1.0 for the post-closure period

In the figure, q is the heat flux from the drift wall; T is the static temperature.

The various boundary conditions for the heat conduction calculations are:

1. The ground surface and the water table boundaries are considered isothermal with the average temperature equal to $25°C$ or $298K$.
2. Through the outer drift wall surface constant heat flux of 23 W/m^2 is applied.
3. The left and right boundaries are considered adiabatic.

The value of the heat flux of 23 W/m^2 is found based on the following. Each canister in the drift has thermal loading equal to 7,284 W. The number of canisters in the drift is equal to 67. So, the thermal loading of one drift is 67×7,284=488,028 W. The area of the drift can be found from A_{drift}=4×5.0×1,061=21,220 m^2. The heat flux is imposed on the drift wall instead of the canister. It can be taken that the drift contains a source of heat of magnitude 488,028W, and the heat is equally distributed to the surface of the drift. Then the heat flux from the drift wall to the rock can be found as q=488,028/21,220=23.00 W/m^2.

Since the CFDHT v.1.0 performs non-dimensional analyses, the boundary conditions as well as the dimensions must be nondimensionalized. In Figure 4-10 below, the dimensionless domain for the heat conduction calculations is shown

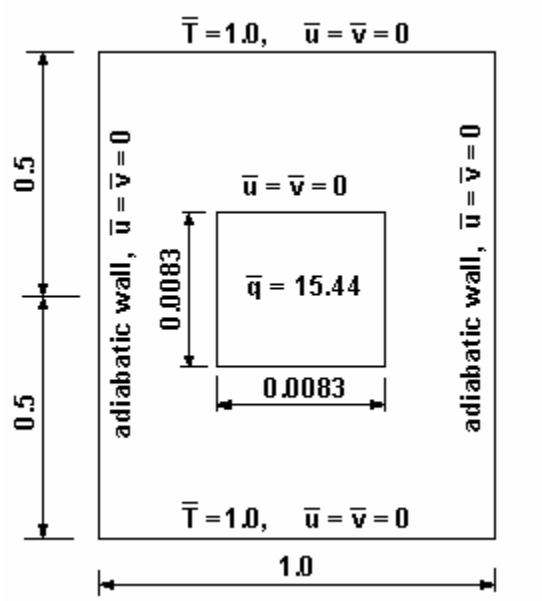

Figure 4-10. Nondimensionalized boundary conditions for the heat conduction through rock calculations using CFDHT v.1.0 for the post-closure period

In the figure, the over bar denotes nondimensionalized parameters. Since CFDHT v.1.0 calculates the heat conduction by means of reducing the energy equation to the heat conduction equation, non-slip boundary conditions must be taken on all boundaries.

The dimensionless boundary temperature and heat flux were found as follows

$$\bar{T}=\frac{T}{T_{top}}=1, \qquad \bar{q}=\frac{q}{\kappa T_{top}/H}=\frac{23.00}{3\cdot 298/600}=15.44$$

where T_{top} is the temperature on the ground surface,

H is the distance between the ground surface and the water table

The dimensionless geometric dimensions were obtained from their dimensional counterparts by dividing the latter by H.

4.1.3 Physical Properties

For the *forced convection* problem, the air properties are taken as

Density of air (ρ): 1.184 kg/m^3
Viscosity (μ): 0.00001855 kg/(m·s)
Specific Heat (C_v): 718.87 J/(kg·K)

For the *natural convection* problem, the last two air properties given on the list above, i.e. viscosity (μ) and specific heat (C_v) are taken as for forced convection problem. The density of the air cannot be taken constant due to compressibility effects caused by the buoyancy in the natural convective system. STAR-CD v.3.150 calculates the density of the air in all mesh points based on the calculated temperature values [9].

For the *heat conduction* problem, the rock is modeled as a continuum with average properties (the approach and the properties of rock were borrowed from Moujaes [3]).

Density of rock (ρ): 2,640 kg/m^3
Thermal Conductivity (κ): κ=3 W/(m·K)
Specific Heat (C_p): 800 J/(kg·K)

4.2 Criteria

There are no specific criteria that are directly applicable to the numerical analysis.

4.3 Codes and Standards

There are no codes or standards directly applicable to the numerical analysis.

5 Assumptions

The assumptions considered in this section make up a part of the process model, which is described in detail in section 6 of this report.

5.1 For the forced convection during the pre-closure period

1. Steady-state solution exists and takes place.

Rationale: Several reasons can be given for using this assumption. The reasons are explained below. First, the waste package heat generation within the Yucca Mountain drift is sufficiently well characterized physically, and the laws of heat decay are based on mathematical relations in the exponential form. However, if only the worst scenario is of principal interest, the heat decay can be neglected. The worst scenario can imply the heat due to some unpredictable barriers in the complex system of the Yucca Mountain repository design does not decay with time. Consequently, heat flux from the waste package is not a function of time. Second, the turbulent forced convective air flow in the Yucca Mountain drift implies the thermal-fluid parameters such as static temperature, velocity, etc in every point within the drift are functions of time. It is an established approach to decompose the parameter to the time-mean value (static in time) and the fluctuating (changing in time) part, and use empirical approach to model the fluctuations so that the process is modeled as time-independent. Third, the forced convective air flow in the Yucca Mountain drift can be modeled as a flow over a series of backward facing steps. This type of problems is known to cause time-dependent oscillations in some circumstances at the location of the reattachment point. The general theory of flows of this type does not exist; it is assumed time-dependent oscillations in the air are not in present. Fourth, the heat

removal from the drift to the rock is assumed negligibly small, and rationales for this assumption will be considered later. Combining the described reasons, i.e. (1) the heat flux is constant due to the worst scenario considerations; (2) the turbulent fluctuations are modeled using methods published in the peer-reviewed literature, i.e. turbulence models (e.g. standard k-ε model); (3) behind the backward-facing step in the Yucca Mountain drift the location of the reattachment point is assumed not changing with time because no direct data to our knowledge are available; (4) the heat removal from the drift to the rock is assumed negligible and the rationales for the approach will be considered later, the fluid flow and heat transfer process in the Yucca Mountain drift during the pre-closure period is modeled as a steady-state process.

2. The canister load is constant throughout the pre-closure period.

Rationale: The reason for using this assumption has been mentioned in the first assumption consideration. The reason is repeated in brief below. Heat from the nuclear waste package to be emplaced to the Yucca Mountain drift decays with time according to the exponential law. If only the worst scenario is of principal interest, the heat decay can be neglected. The worst scenario can imply the heat due to some unpredictable barriers in the complex system of the Yucca Mountain repository design does not decay with time. Consequently, the heat flux and the canister load in the Yucca Mountain drift are constant throughout the pre-closure period.

3. Gravitational forces have no effect on the flow.

Rationale: Actual parameters, such as pressure, velocity and static temperature, are complex functions of the drift geometry, roughness of the drift wall, body forces, etc are subject to the solution of the fundamental equations of the fluid dynamics and heat transfer. Because a general model for these effects does not exist, and the Yucca Mountain drift will occupy a horizontal position, and the speed of the ventilating air will be considered high enough to carry away falling down due to gravity air particles, the gravity force can be neglected in the approximation.

4. All the canisters are of the same size and the same load.

Rationale: This is an established approach in the peer-reviewed literature, which is close to the real case situation and allows significant simplification of the model.

5. The distribution of heat flux from the canister over the canister surface is uniform.

Rationale: This is also an established approach in the peer-reviewed literature, which is close to the real case situation and allows significant simplification of the model.

6. The heat transfer to the rock is a path of higher resistance than that to the ventilating air, and therefore negligible, and the walls of the drift and the floor are therefore adiabatic.

Rationale: Because a general model for heat transfer and fluid flow in the Yucca Mountain drift in the pre-closure period is not well established to our knowledge, the effects of heat removal from the drift via conduction through the rock in the pre-closure period are not documented in detail in the open literature. The adiabatic walls will be considered as a reasonable approximation for the forced convective flow situation in the Yucca mountain repository in the pre-closure period.

7. Radiation heat transfer can be neglected.

Rationale: Because a general model for heat transfer and fluid flow in the Yucca Mountain drift in the pre-closure period is not well established to our knowledge, the effects of radiation heat transfer from the canister surface to the air in the pre-closure period are not well documented in the open literature. Therefore, based on the assumption that the temperature on the canister surfaces will be low enough in the pre-closure period due to the forced ventilation system, the adiabatic walls will be

considered as a reasonable approximation for the thermal situation in the Yucca mountain drift during the pre-closure period.

8. The uniform distribution of the ventilating air takes place at the inlet.

Rationale: Because the ventilation system to be used in the pre-closure period for cooling canisters emplaced in the Yucca Mountain drift is not yet established, then for the simplification purpose the uniform distribution of the ventilating air at the inlet to the Yucca mountain drift during the pre-closure period is considered.

5.2 For the natural convection during the post-closure period

1. Steady-state solution exists and takes place

Rationale: Several reasons given above for the explaining of using this assumption for the pre-closure period can be used for the post-closure period as well.

2. The canister load is constant throughout the post-closure period and equal to the load of the pre-closure period.

Rationale: Several reasons given above for the explaining of using this assumption for the pre-closure period can be used for the post-closure period as well.

3. The distribution of heat flux from the canister over the canister surface is uniform.

Rationale: Several reasons given above for the explaining of using this assumption for the pre-closure period can be used for the post-closure period as well.

4. The heat transfer to the rock takes place.

Rationale: The heat transfer to the rock in the post-closure period cannot be neglected as it was done for the pre-closure period. As the forced ventilation is off, the heat path through the rock is the only path for removal of heat from the Yucca Mountain repository in the post-closure period.

5. Radiation heat transfer can be neglected.

Rationale: Several reasons given above for the explaining of using this assumption for the pre-closure period can be used for the post-closure period as well.

6. The walls of the drift and the floor are isothermal with the uniform temperature distribution.

Rationale: Because a general model for heat transfer and fluid flow in the Yucca Mountain drift in the post-closure period is not well established to our knowledge, the temperature distribution on the drift wall is not known a priori. Isothermal wall assumptions are taken due to the consideration that the temperature on the wall in the post-closure period will be maintained constant due to the heat transfer to the rock.

5.3 For the heat conduction during the post-closure period

1. Steady-state solution exists and takes place

Rationale: Several reasons can be given for using this assumption. Most of the reasons are identical to those for the forced convection during the pre-closure period. Here is a summary of the reasons: (1) the heat flux from the waste package is constant due to the worst scenario considerations; (2) the turbulent fluctuations of the natural convective flow inside the drift are modeled using methods published in the peer-

reviewed literature, i.e. turbulence models (e.g. standard k-ε model); (3) the temperature on the ground surface and water table is maintained constant due to natural conditions.

2. The drifts at the emplacement area have no effect on each other, and therefore one drift can be considered separately from the others.

Rationale: Because a general model for heat transfer through the Yucca Mountain rock does not exist to our knowledge, for simplification purposes one drift is considered perfectly isolated from the other drifts.

3. The drift is a uniform source of heat with the heat flux on the drift wall calculated based on the thermal loading of 67 canisters located inside the drift.

Rationale: This is a common approach in the peer-reviewed literature (e.g. Moujaes)

4. The thermal loading of canisters and therefore the heat flux from the drift wall to the rock is constant throughout the post-closure period and equal to the loading of the pre-closure period.

Rationale: The assumption is based on the worst scenario considerations.

5. The temperature of the rock on the ground surface and the water table layer is constant throughout the year and equal to 25 °C. Note: the Topopah Spring Tuff contains the Repository Host Horizon (RHH). The ambient rock temperature in the RHH is 26.1°C. This information is based on CRWMS M&O 1999b, Table 6-3, p.34. This value of the ambient rock temperature, i.e. 26.1°C is close to the value used by Mojaes and in this report, i.e. 25°C.

Rationale: This is an established value in the peer-reviewed literature (e.g. Moujaes). However, data exist about the ambient rock temperature in the Topopah Spring Tuff, which is 26.1°C. This information is located at CRWMS M&O 1999b, Table 6-3, p.34. This value of the ambient rock temperature, i.e. 26.1°C is close to the value used by Moujaes and in this report, i.e. 25°C. The correction of the value should negligibly affect the analysis.

6. The vertical boundaries of the computational domain are located far enough from the heat generating drift wall, and therefore they are adiabatic.

Rationale: The assumption that the vertical walls are adiabatic is primarily based on the assumption made earlier that the drifts at the emplacement area have no effect on each other. In this condition, the vertical boundaries must be located far enough from the drift to eliminate the influence of the heat accumulation on the vertical boundaries due to the perfect insulation of the boundaries on the drift wall temperature.

7. Rock at the Yucca Mountain is a continuum with average properties.

Rationale: This is an established approach in the peer-reviewed literature (e.g. Moujaes).

All of these assumptions will be used in section 6 of this report.

6 Analysis/ Model

6.1 Description of the CFDHT model

6.1.1 Introduction

The design of the canisters to be used for the long-term storage of high-level nuclear waste has progressed from the borehole model indicated in the original site characterization plan for the Yucca Mountain repository program to the drift emplaced multipurpose containers. These containers may contain 21 or more pressurized water reactor fuel assemblies. The zirconium alloy cladding and uranium oxide fuel pellets make up the fuel assemblies.

Removal of heat is important if the zircaloy cladding degradation temperature of 350°C is not to be exceeded. Above this temperature, the oxide layer on the zircaloy cladding grows continuously leading to early failure. Operation of the repository is currently planned in two periods of time – pre-closure (before repository closure) and post-closure (after repository closure). In the pre-closure drift system, air ventilation will provide forced convection cooling of the canister walls that will remove decay heat. In the post-closure drift system, air ventilation will be discontinued and the heat will be removed from the canister surface by natural convection.

The proper design of the required repository ventilation system must be based on knowledge of the heat transfer flow patterns between the canister surface and the drift wall. Convective heat transfer from the canisters may be determined through appropriate computer models. In this sixth section of the report we will introduce a new ventilation model, CFDHT, for both pre-closure and post-closure periods. The model will be used to assess the performance of the proposed repository system both in the pre-closure and post-closure periods by analyzing the maximum temperature in the drift at the real case conditions, locations of hot spots in the drift, and required ventilation speed of the air.

Then, we will give validation of the model at the end.

6.1.2 CFDHT model for the pre-closure period

6.1.2.1 Forced Convection

The dimensions of the drift are shown in Figure 4-1. The dimensions are taken from the peer-reviewed literature (Danko, 1995). Of the required 67 canisters in the drift and the total length of 1,061 m we considered a part of the

length, which included only 46 canisters for modeling the sequence of canisters in the drift. In the CFDHT model for the pre-closure period, we insulated the temperature calculation in the drift from the calculation of the surrounding rock, which corresponds to the worst scenario of the waste storage when heat cannot be removed from the repository through the rock and the drift wall temperature increases significantly due to the heat transfer from the air. The ventilating air enters the drift from the left and exits from the right. Only a small amount of heat reaches the wall of the repository via the air by convection, thus the drift wall remains cool. Since the drift is insulated in this study, we only consider one drift assuming the situation in the other drifts to be similar.

As we are considering ventilation, all the heat is carried away from the canisters by the ventilating air. The cooling of canisters by the air reduces the temperature on the canister surface significantly, depending on air speed at the inlet, thereby making the radiation heat transfer from the canister to the drift wall negligibly small. The ventilating air flow in the drift is highly turbulent. The modeling is carried out using STAR-CD v. 3.150, well known commercial Computational Fluid Dynamics (CFD) software. In addition STAR-CD v. 3.150 was benchmarked for Yucca Mountain work. The input parameters described in section 4, Inputs, are taken from the databases of STAR-CD v.3.150, which was benchmarked for Yucca Mountain work and peer-reviewed literature, and this helps to build confidence in the model.

6.1.3 CFDHT Model for the Post-Closure Period

6.1.3.1 Natural Convection

Of the required 67 canisters in the drift and the total length of 1,061 m for natural convection calculations in the post-closure period we considered a part of the length, which included only 3 canisters for modeling the sequence of canisters in the drift. During the post-closure period, the forced ventilation is off, and the

heat can be removed from the drift only through the rock. Thus, in this model for the post-closure period, the temperature calculation in the drift was coupled with the heat conduction calculation through the surrounding rock through the temperature boundary condition. The calculation of heat conduction through the rock performed using the CFDHT v. 1.0 software gave the temperature boundary condition for the drift wall, which was used for calculation of natural convection in the drift. The free convective air flow in the Yucca Mountain drift is highly turbulent. The modeling of natural convection is carried out using STAR-CD v. 3.150. The input parameters described in section 4, Inputs, are taken from the databases of STAR-CD v.3.150, which was benchmarked for Yucca Mountain work and peer-reviewed literature, and this helps to build confidence in the model.

6.1.3.2 Heat Conduction

The purpose of the calculation of heat conduction through the rock is to provide a boundary condition for temperature on the drift wall for STAR-CD v.3.150 simulation of natural convection during the post-closure period. The computational domain with geometric dimensions shown in figures 4-3 and 4-4 was approximated as a two-dimensional area of the square shape with various types of boundary conditions on horizontal and vertical boundaries. The horizontal boundaries of the computational domain were moved far away from the drift to the locations, where the temperature is maintained constant due to natural conditions. Such locations are the ground surface and the water table levels. On the ground surface level the temperature changes of the rock throughout the year were neglected, and the average annual temperature instead was used for calculations. Temperature on both the ground surface and water table was taken equal to 25°C. The vertical boundaries of the computational domain were also moved far away from the drift to the locations where the change of temperature in the horizontal direction could be neglected. Based on the

geometry independent analysis, the locations for the vertical boundaries were chosen as 300 m to the left and 300 m to the right of the drift center. The difference in computed temperature on the drift wall for the locations of the horizontal boundaries 150 m and 300 m was 5.5 %, whereas the difference in calculated temperature on the drift wall for the locations 300 m and 600 m was roughly twice smaller, i.e. only 2.5%. Thus, the location 300 m proved to be a good location for the vertical boundaries.

The modeling of heat conduction was carried out using CFDHT v.1.0 software that performs 2-D finite element steady-state incompressible thermal-fluid analysis based on solving momentum and energy equations in the dimensionless form. The heat conduction equation is solved by CFDHT v.1.0 by means of reducing the energy equation to the heat conduction equation. The CFDHT v.1.0 was benchmarked for Yucca Mountain work. The computational mesh used for the analysis is shown in Figure 4-6. Since the drift diameter is significantly smaller than the height and the width of the domain, the circular cross section of the drift was approximated by only one finite element of a square shape located in the center of the mesh as shown in Figure 4-6. The dimensionless heat flux imposed for all four sides of the element was based on the thermal loading of canisters at the time of emplacement. The computational domain with boundary conditions in the dimensionless form is shown in Figure 4-10. The found dimensionless values of temperature were converted to dimensional values by multiplying them by the temperature on the ground surface, i.e. 298 *K*. The rock at the Yucca Mountain is modeled as continuum with average properties. The input parameters described in section 4, Inputs, are taken from the peer-reviewed literature such as scientific journals, and this helps to build confidence in the model.

6.2 Application of the CFDHT model

6.2.1 Pre-Closure Period

Two speeds of the ventilating air at the inlet were considered, i.e. $w_{in} = 1 m/s$ and $w_{in} = 1.5 m/s$. The Reynolds number for the two cases:

for $w_{in} = 1 m/s$:

$$\mathrm{Re} = \frac{\rho \cdot w_{in} \cdot D}{\mu} = \frac{1.184 \cdot 1.0 \cdot 5.0}{0.00001855} = 319{,}137$$

for $w_{in} = 1.5 m/s$:

$$\mathrm{Re} = \frac{\rho \cdot w_{in} \cdot D}{\mu} = \frac{1.184 \cdot 1.5 \cdot 5.0}{0.00001855} = 478{,}706$$

Hence the flow is highly turbulent, and the standard k-ε turbulence model [5] was used for the STAR-CD v.3.150 simulation [8].

Only one computer run was required to analyze the temperature and velocity distribution in the drift at the forced convection conditions during the pre-closure period for each of the considered speeds of the ventilating air, i.e. 1 m/s and 1.5 m/s. The STAR-CD v.3.150 was run until solution reached convergence to the designated tolerance 0.001. The fact that the solution converged builds confidence in the model. No run non-convergences were observed.

The results of the run were imported to Tecplot v.9.2-0-3, which was used for post-processing.

The temperature contours from Tecplot for three canisters, namely canister 1, 23, 46 are shown for the inlet velocity 1 m/s in Figures 6-1, 6-2, 6-3, for inlet velocity 1.5 m/s in Figures 6-4, 6-5, 6-6.

1.0 m/s

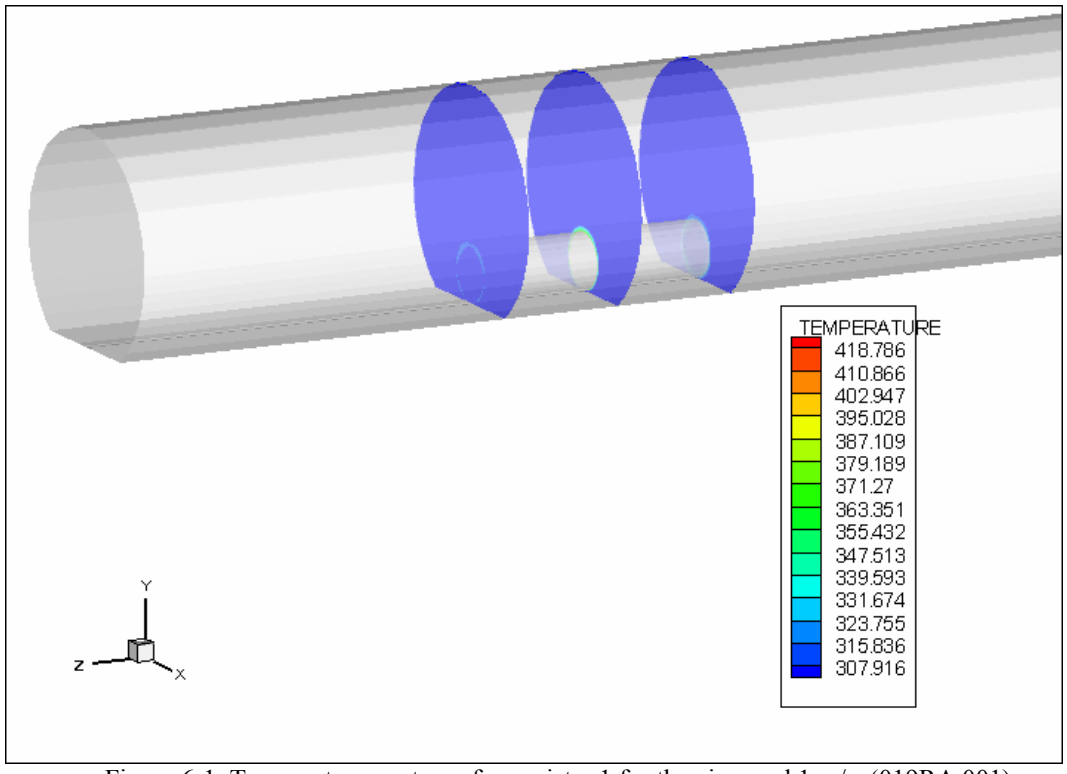

Figure 6-1. Temperature contours for canister 1 for the air speed 1 m/s. (019RA.001)

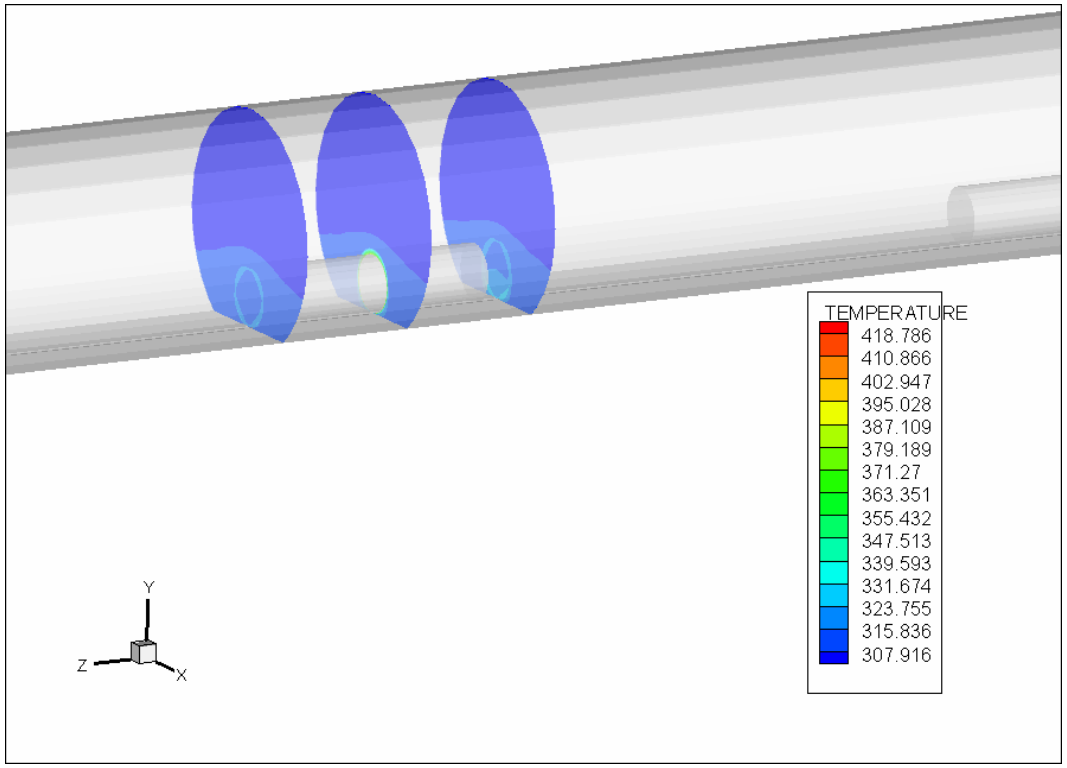

Figure 6-2. Temperature contours for canister 23 for the air speed 1 m/s. (019RA.001)

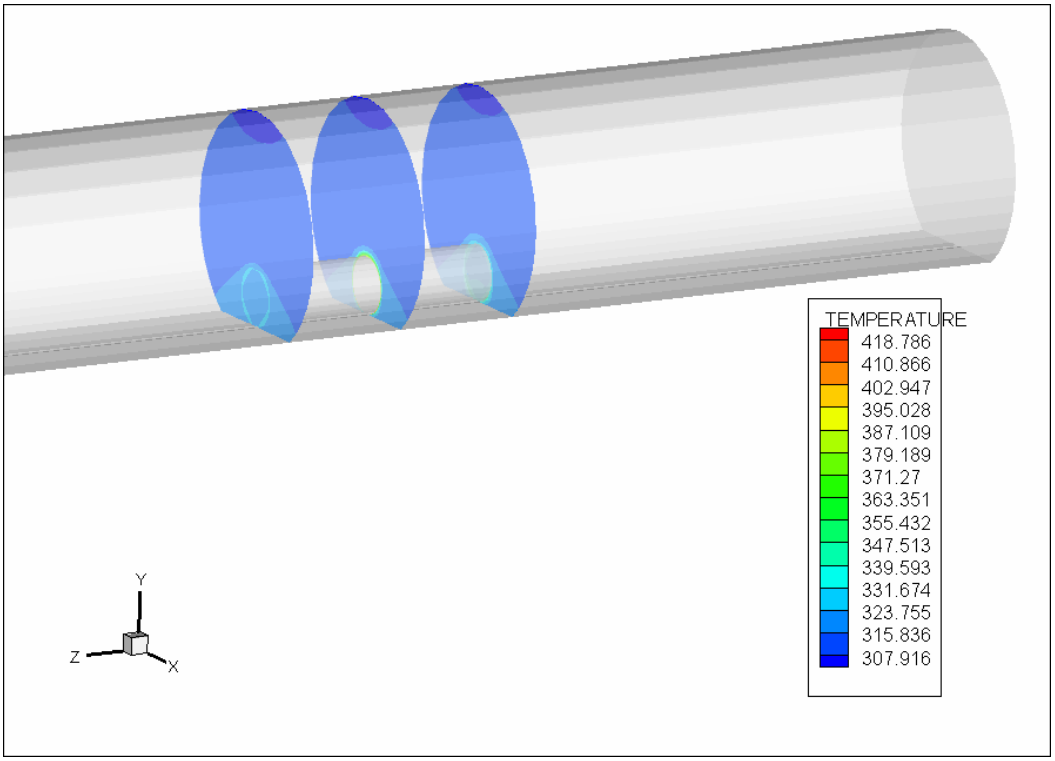

Figure 6-3. Temperature contours for canister 46 for the air speed 1 m/s. (019RA.001)

1.5 m/s

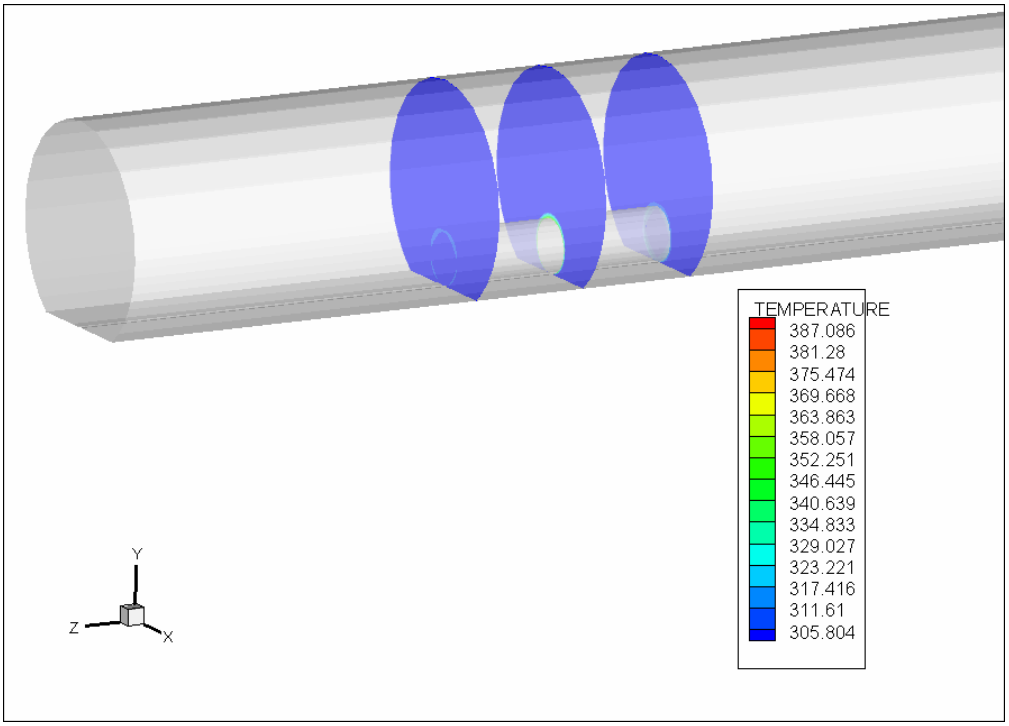

Figure 6-4. Temperature contours for canister 1 for the air speed 1.5 m/s. (019RA.001)

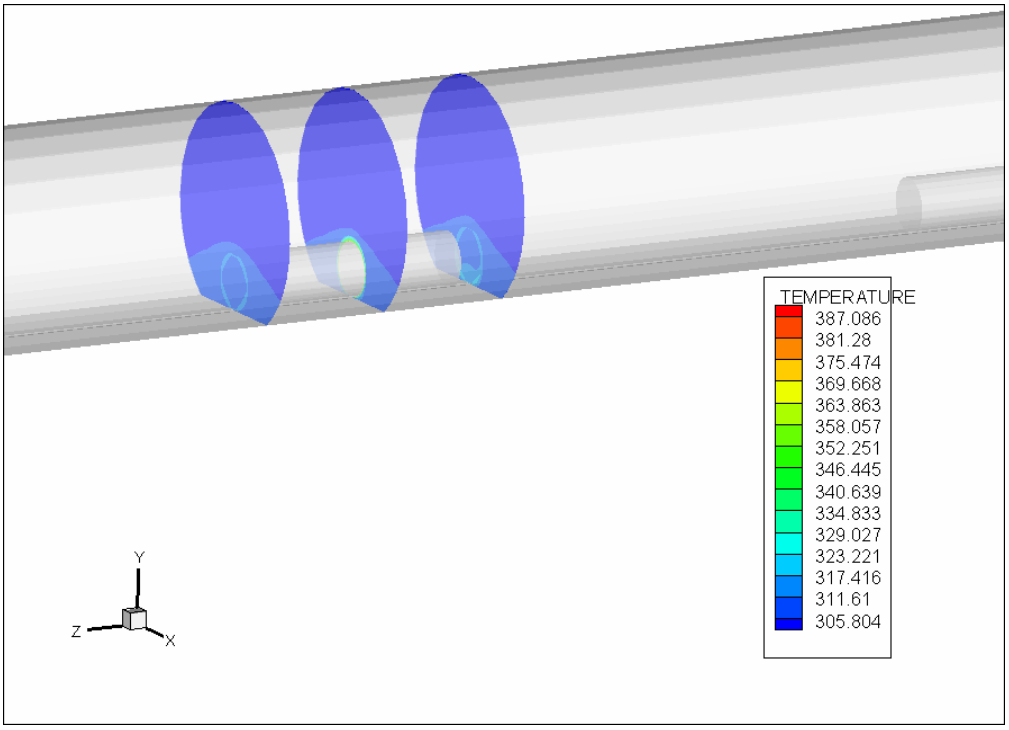

Figure 6-5. Temperature contours for canister 23 for the air speed 1.5 m/s. (019RA.001)

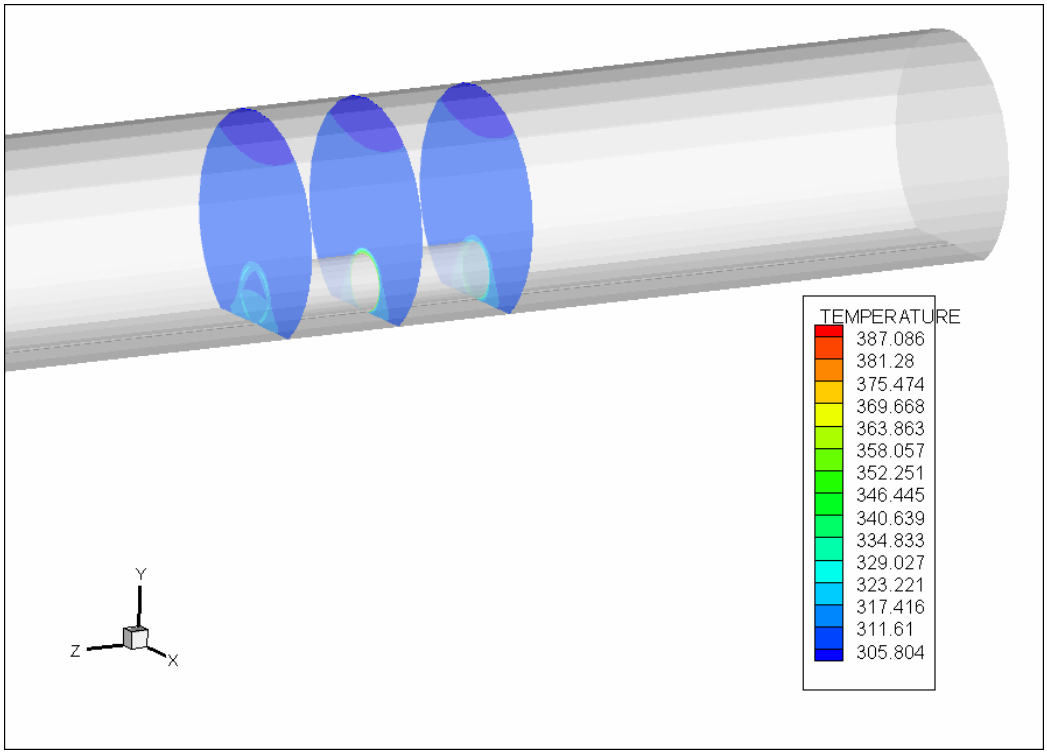

Figure 6-6. Temperature contours for canister 46 for the air speed 1.5 m/s. (019RA.001)

6.2.2 Post-Closure Period

The Rayleigh number based on the Yucca Mountain drift dimensions, air properties at the reference temperature, and the acceleration due to gravity is of order 10^{12}, so the free (natural) convective air flow during the post-closure period in the drift is highly turbulent. The standard k-ε model was used for the STAR-CD v.3.150 simulations.

Only one computer run was required to analyze the temperature and velocity distribution in the drift at the natural convection conditions during the post-closure period. The STAR-CD v.3.150 was run until solution reached convergence to the designated tolerance 0.001. The fact that the solution converged builds confidence in the model. No run non-convergences were observed.

The results of the run were imported to Tecplot, which was used for post-processing. Temperature contours and velocity vectors from Tecplot are shown in Figures 6-7, 6-8, 6-9.

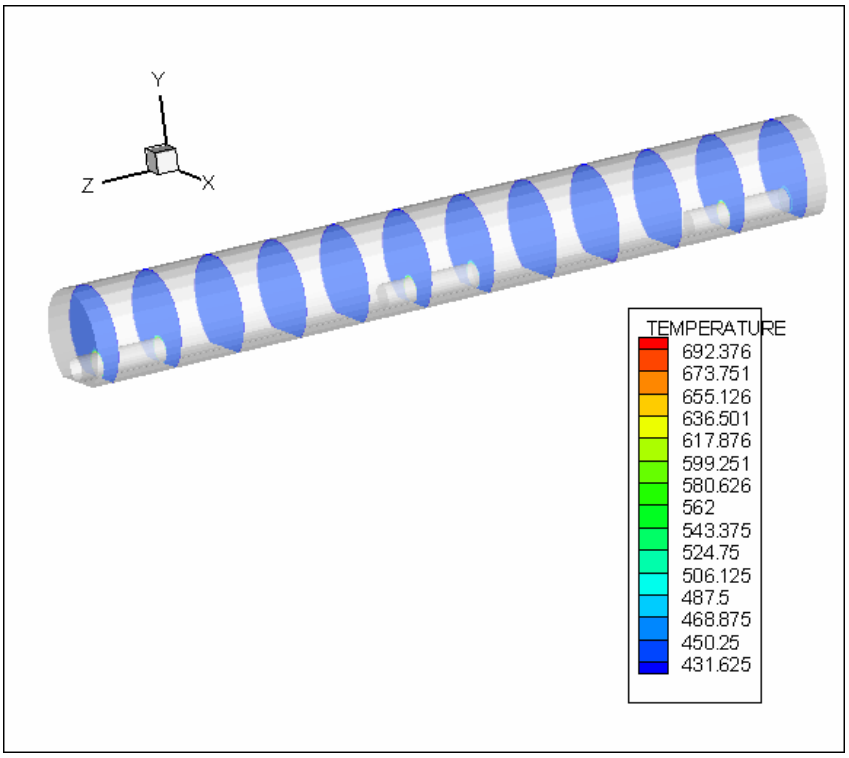

Figure 6-7. Temperature contours in cross sections of the drift for natural convection calculations (019RA.001)

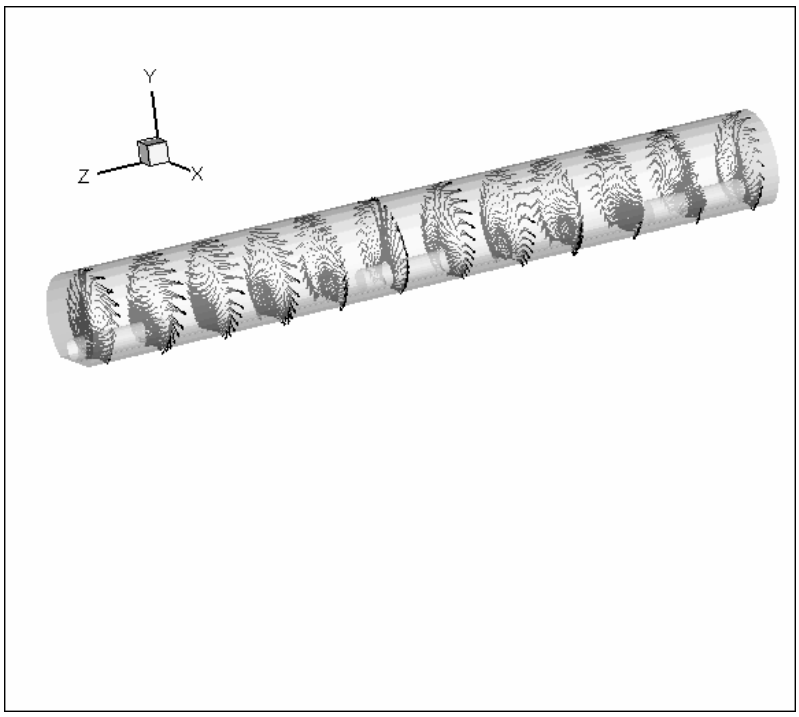

Figure 6-8. Velocity vectors in cross sections of the drift for natural convection calculations (019RA.001)

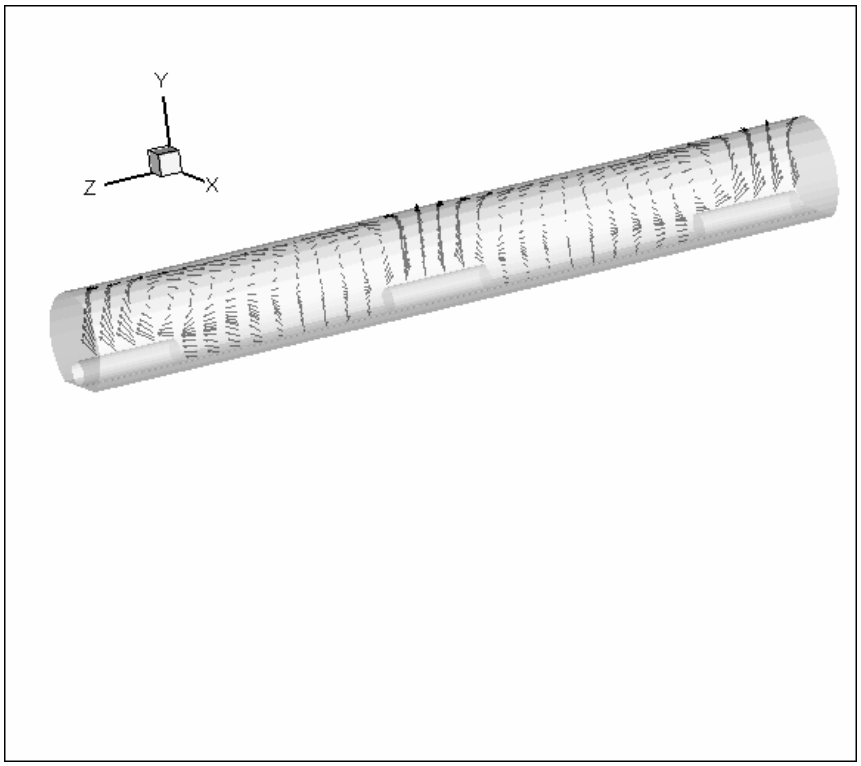

Figure 6-9. Velocity vectors in the longitudinal section passing through the drift axis for natural convection calculations (019RA.001)

Only one computer run was required to analyze the temperature distribution in the rock during the post-closure period. The CFDHT v.1.0 was run until solution reached convergence to the designated tolerance 1×10^{-9}. The fact that the solution converged builds confidence in the model. No run non-convergences were observed.

In Figure 6-10 the dimensionless temperature in the rock contours obtained using the CFDHT v.1.0 code for the heat conduction through the rock calculations are given. The values on the legend must be multiplied by 298 to get the dimensional temperature values. The plots are performed using the Tecplot software.

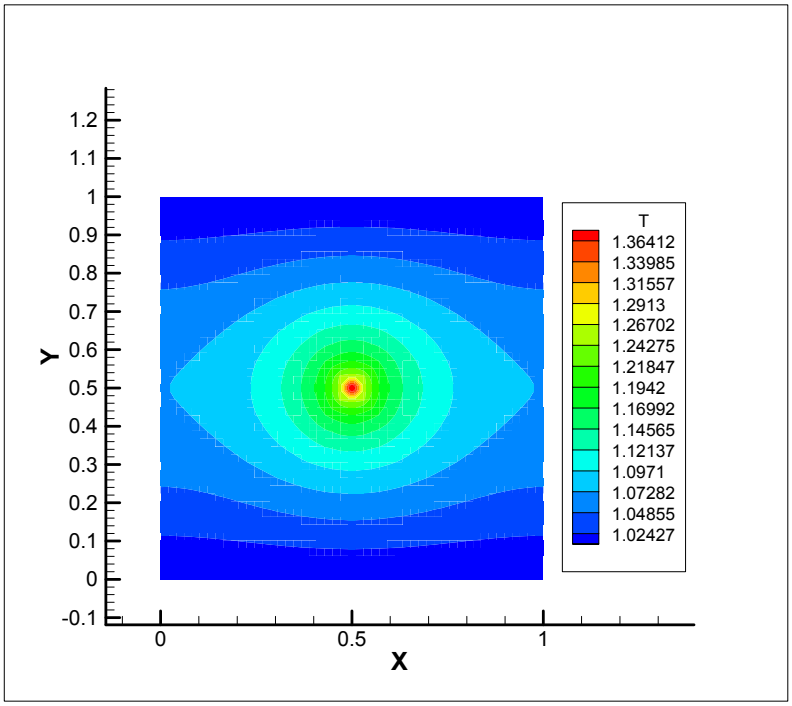

Figure 6-10. The temperature distribution in the mountain rock during the post-closure period (019RA.001)

6.3 Validation of the CFDHT model

Model validation has been accomplished following guidelines cited in QAP 3.3 procedure (section 4.2). Validation of model means the model can account for all available data. In this model report, published data available from the open scientific literature [6-8] have been used to validate mathematical

models to predict velocity and temperature distribution inside the drift during the pre-closure and post-closure periods. The model predicted values showed satisfactory agreement with the experimental data. Alternative approach such as comparing model predicted values with analytical solutions for the heat conduction calculations (section 6.3.2.2) helped improve the level of confidence in the model. Discussion of potential sources of error and the impacts of input uncertainties to model results is given in Section 7 of this report. References to the supporting information needed to substantiate the model validation are given in section 8 of this report under numbers [6-8, 11-14].

The criteria used to establish the adequacy of the scientific basis for the CFDHT model are 25% for comparisons of the model output with experimental data, and 5% for comparisons of the model output with analytical solutions. The quantitative criteria of 25% for comparisons with experimental data are based on the fact that experimental data themselves are not accurate, and the uncertainty of the experimental data is usually taken as 25%. For comparisons with analytical solutions, where the uncertainty is 0%, the quantitative criteria must be stricter, and the allowable discrepancy of numerical results and analytical solutions is usually taken as 5% to allow minor discretization errors in the numerical analysis to be accounted. Consequently, the model is sufficiently accurate for its intended use, which is to determine the velocity and temperature distribution in the drift along with the highest temperature, and consistent with parameter uncertainties, if the output from the model satisfies criteria described above.

The post-development validation of the mathematical model is corroborated by using specified pre-test model predictions (available in the open literature experimental data for forced convection [6] and natural convection [7,8] and analytical estimates for the heat conduction) to specified data collected during the associated testing. Details of the testing are described in sections 6.3.1.1, 6.3.2.1 and 6.3.2.1.

6.3.1 Pre-Closure Period

6.3.1.1 Forced Convection

The STAR-CD v.3.150 software was used to perform an analysis of the turbulent forced convection phenomenon during the pre-closure period. The software was benchmarked for Yucca Mountain work. The description of the test case of forced convection is given in Section 3 of the Software Definition Report (SDR) with the Software Baseline Documentation Number UCCSN-SDR-002. The results of the validation could be found in section 2 of the Software Implementation Report (SIR) with the Software Baseline Documentation Number UCCSN-SIR-002. Numerical results for the test are attached on a CD-ROM disk to the UCCSN-SIR-002 as appendix 1. Here is the short description of the test and numerical results

Test (Heat Transfer in a Pipe Expansion)

This problem involves two-dimensional turbulent flow with convective heat transfer. In this problem, a fluid is injected into an axisymmetric pipe that has a downstream expansion. The fluid in the pipe is heated through the expansion pipe walls. The main purpose of this test is to test the ability of STAR-CD v. 3.150 and the CFDHT model to accurately predict heat transfer and turbulence. The test problem provides a test of STAR-CD v. 3.150's ability to transport heat convectively. During the repository's pre-closure period, heat will be transported principally by forced convection. Thus, this test problem provides a useful test for STAR-CD v. 3.150 and the CFDHT ventilation model. Baughn et al. (1984) provides experimental data for this test.

Here are some details of the test. The left end of the pipe, which is the pipe inlet, has a diameter of 1.33 m. At 1 m downstream from the pipe inlet the pipe diameter instantaneously expands to 3.33 m. The length of this expanded section of the pipe is 40 m. The fluid properties are constant. The fluid density is 1 kg/m^3, the fluid dynamic viscosity is 1×10^{-05} Pa·s, the fluid thermal conductivity is $1\times l0^{-04}$ W/m·K, and the fluid specific heat is 0.7 J/kg·K. The inlet fluid velocity and turbulence parameters (k-ε) are calculated from profiles of fully developed turbulent flow in a

pipe. A pressure outlet boundary condition is used at the expanded pipe outlet on the right side of the pipe. The boundary condition along the expanded section of the pipe is a uniform heat flux of 0.3 W/m^3. The smaller section of pipe and the left face of the expanded section are fully insulated. The fluid temperature at the pipe inlet is 273 K. Standard k-ε model of turbulence was used.

Plots of a normalized Nusselt number along the expanded pipe wall are required for this problem. The normalized Nusselt number is calculated as follows:

$$Nu_N(x) = \frac{Nu(x)}{Nu_{DB}}$$

$$Nu(x) = \frac{h(x)D}{k}$$

$$Nu_{DB} = 0.023\,\mathrm{Re}^{0.8}\,\mathrm{Pr}^{0.4} = 97.24$$

$$\mathrm{Re} = \frac{4\dot{m}}{\pi\mu D} \cong 40750$$

$$\mathrm{Pr} = \frac{C_p\mu}{k} = 0.7$$

$$h(x) = \frac{q''}{T_{Wall}(x) - T_B(x)}$$

$$T_B(x) = \frac{4q''x}{\mathrm{Re}\,\mu C_p} + 273$$

where Nu_N is the normalized Nusselt number, Nu is the local Nusselt number, Nu_{DB} is the fully-developed Nusselt number as defined by the Dittus-Bolter formula, Re is the

Reynolds number, Pr is the Prandtl number, D is the diameter of the expanded pipe section, T_{wall} is the temperature along the expanded pipe wall, T_B is the bulk temperature, c_p is the specific heat of the fluid, k is thermal conductivity of the fluid, h is the heat transfer coefficient, $\dot{m}$ is the mass injection rate (10.64 kg/s), q'' is the heat flux along the expanded pipe wall, c is distance along the expanded pipe, ρ is the fluid density, and μ is the fluid dynamic viscosity. The results should be compared to the normalized Nusselt number from experimental data as provided for the Reynolds number curve of 40,750 presented in Figure 4 of Baughn's article (1984) and summarized in Table 6 of the same article. For acceptance, the difference between the STAR-CD v. 3.150 calculated normalized Nusselt numbers and the experimental values must be within 25 percent of the range.

Input and output files are lengthy and are stored on the validation test CD-ROM that is attached to the SIR report as Attachment 1. The files are listed in Section 2.5 of this SDR report. Acceptance criteria for this part of the test case are based on STAR-CD v. 3.150 results being within specified range of the experimental values for the normalized Nusselt number downstream from the pipe expansion, as established in Table 6 of the STAR-CD v. 3.150 Software Definition Report. Because it is difficult to grid computational fluid dynamics problems to correspond with points of experimental values, the experimental results were converted to curves in the figures below. Upper and lower bounds of the acceptance bands, as based on the acceptance criteria, are also shown in the figures. If the STAR-CD v. 3.150 results plot between the upper and lower acceptance bands, then STAR-CD v. 3.150 passes that particular test.

Figure 6-11 shows a plot of the normalized Nusselt number downstream from the pipe expansion for the standard k-ε turbulence-model. The acceptance band criterion is based on Table 6 of the STAR-CD v. 3.150 SDR. The figure shows the STAR-CD v. 3.150 results along with the experimental results and the acceptance band. The STAR-CD v. 3.150 results are within the acceptance band at all points with experimental data.

The figure shows that the STAR-CD v. 3.150 results are within the acceptance bands. Therefore, STAR-CD v. 3.150 passes the acceptance criterion for this test case as defined in Section 3.4.6 of the STAR-CD v. 3.150 SDR.

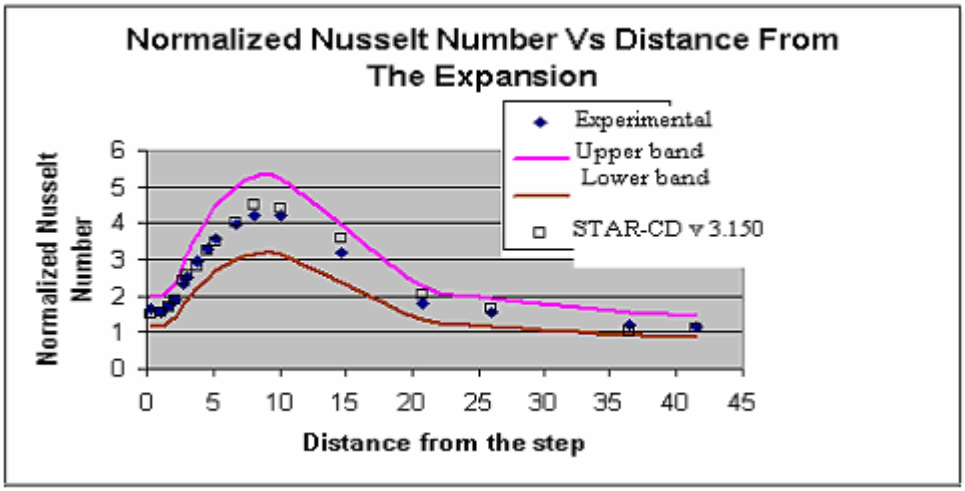

Figure 6-11. Normalized Nusselt Number vs Distance from the Expansion (UCCSN-SIR-002)

6.3.2 Post-Closure Period

6.3.2.1 Natural Convection

The STAR-CD v.3.150 software was used to perform an analysis of the natural convection phenomenon during the post-closure period. The software was benchmarked for Yucca Mountain work. The description of the test case of natural convection is given in Section 3 of the Software Definition Report (SDR) with the Software Baseline Documentation Number UCCSN-SDR-002. The results of the validation could be found in section 2 of the Software Implementation Report (SIR) with the Software Baseline Documentation Number UCCSN-SIR-002. Numerical results for the test are attached on a CD-ROM disk to the UCCSN-SIR-002 as appendix 1. Here is the short description of the test and numerical results

Test (Natural Convection in an Annulus)

This is a test of heat-induced two-dimensional, natural convection in a hollow cylindrical annulus. This test provides a good test of STAR-CD v. 3.150's ability to convect heat under natural convection. In a crude sense, this test problem simulates natural convection of a two-dimensional cross-section of a heated waste canister in a drift. The test problem is described in Kuehn and Goldstein (1976, 1978).

A solid cylinder of radius 17.8 mm is located in the center of a hollow cylinder of radius 46.3 mm. The cylinders are located in the horizontal plane so that gravity can have an impact on the flow field. The cylinder's cross-sections are modeled in two-dimensions. The surface temperature of the inner cylinder is held at 373 K and the surface temperature of the outer cylinder is held at 327 K. No-slip velocity boundary conditions are applied at the cylinder surfaces. Air is the fluid in the annulus. Except for density, the air's properties are constant with the following values: dynamic viscosity = 2.081×10^{-5} Pa·s, thermal conductivity = 0.02967 W/m·K, specific heat = 1008 J/kg·K and molecular weight = 28.966. The ideal gas law provides the air density. Gravitational acceleration is 9.81 m/s^2, pointing downward. The test problem is run to steady-state conditions and a steady-state solution is desired. The origin of the axes is at the center of the larger cylinder.

For comparison purposes, the following are desired:

- Temperature profile along the vertical axis of symmetry below inner cylinder
- Temperature profile along the vertical axis of symmetry above inner cylinder.

The temperature results for this case shall be compared with the experimental results presented in dimensionless form of Figure 15 of Kuehn and Goldstein's article (1976). The distance and temperature results from Kuehn and Goldstein are converted from the dimensionless distances and temperature and summarized in Table 1 and Table 2 below for the $\theta=0$ and $\theta=180$ curves, respectively, of Figure 15 of Kuehn and Goldstein's article (1976).

For acceptance, the difference between the calculated temperatures and the measured temperatures should be within 10 percent of the expected range of the temperatures, i.e.,

$$\left|T_p - T_m\right| < 0.25\left|T_{\max} - T_{\min}\right|$$

Where, T_m, T_{max}, T_{min}, and T_p are the measured, maximum, minimum and predicted temperatures, respectively. The maximum and minimum temperatures are the temperatures assigned as boundary conditions, 373 K and 327 K on the inner and outer cylinders, respectively. All temperatures should be within this range.

Table 1 Temperatures along Vertical Line of Symmetry below Inner Cylinder (UCCSN-SDR-002)

Vertical Distance From Center Of Outer Cylinder (mm)	Temperature (K)	Location
-18.5	365.3	Below bottom
-19.1	358.6	
-19.9	352.0	
-20.6	345.7	
-21.7	339.6	
-23.6	333.8	
-26.2	330.8	
-30.1	329.2	
-34.6	328.1	
-38.6	327.6	Above bottom

Table 2 Temperatures along Vertical Line of Symmetry above Inner Cylinder (UCCSN-SDR-002)

Vertical Distance From Center Of Outer Cylinder (mm)	Temperature (K)	Location
19.8	371.2	Above top
22.5	367.3	
26.9	363.4	
41.9	359.1	

43.3	355.5	
43.9	351.8	
44.4	348.3	
44.7	344.8	
45.1	341.4	
45.4	338.3	
45.9	331.3	Below top outer

Since this test is a validation of the models in STAR-CD v. 3.150, the STAR-CD v. 3.150 results should be qualitatively similar to the experimental results. Thus, temperature comparisons between the STAR-CD v. 3.150 results and the experimental results should be similar; the trends in temperature with the respect to distance should be similar. This test shows the adequacy of the models implemented in STAR-CD v. 3.150. Because it is difficult to account for all physics in a real system, the tester should not expect the STAR-CD v. 3.150 results to reproduce the experimental results perfectly.

Since it is difficult to grid computational fluid dynamics problems to correspond with points of experimental values, the experimental results were converted to curves in the figures below. Upper and lower bounds of the acceptance bands, as based on the acceptance criteria, are also shown in the figures. If the STAR-CD v. 3.150 results plot between the upper and lower acceptance bands, then STAR-CD v. 3.150 passes that particular test.

Figure 6-12 shows a plot of the temperature along the vertical line of symmetry below the inner cylinder. The acceptance band criterion is based on Table 4 of the STAR-CD v. 3.150 Software Definition Report. The figure shows the STAR-CD v. 3.150 results along with the experimental results and the acceptance band. The STAR-CD v. 3.150 results are located within the acceptance band at all points with experimental data. Therefore, STAR-CD v. 3.150 and the CFDHT model passes this part of the acceptance criteria. Figure 6-13 shows a plot of the temperature along the vertical line of symmetry above the inner cylinder. The acceptance band criterion is based on Table 5 of the STAR-CD v. 3.150 Software Definition Report. The figure shows the STAR-CD v. 3.150

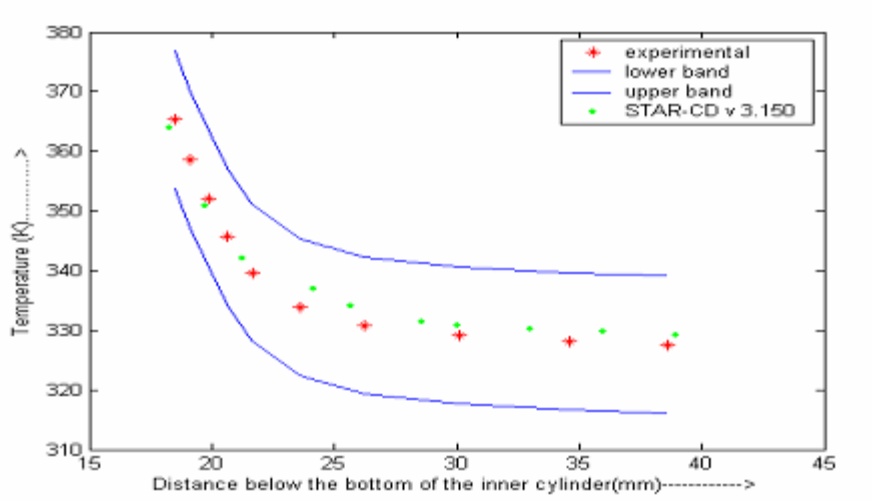

Figure 6-12. Temperature along the vertical line of symmetry below inner cylinder (UCCSN-SIR-002)

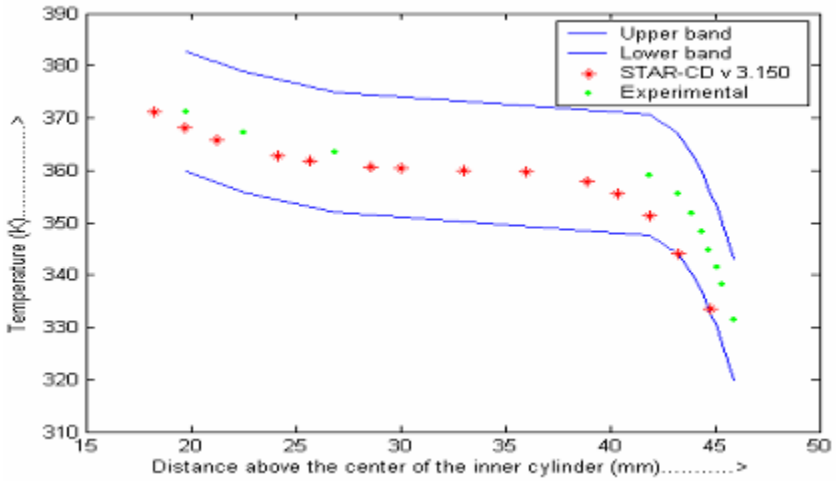

Figure 6-13. Temperature along the vertical line of symmetry above inner cylinder (UCCSN-SIR-002)

results along with the experimental results and the acceptance band. The STAR-CD v. 3.150 results are located within the acceptance band at all points with experimental data. Therefore, STAR-CD v. 3.150 passes the acceptance criterion for this test case as defined in Section 3.4.6 of the STAR-CD v. 3.150 Software Definition Report.

6.3.2.2 Heat Conduction

The CFDHT v.1.0 software was used to calculate the heat conduction through rock problem. The software was benchmarked for Yucca Mountain work. The description of the test case for the heat conduction problem is given in Section 3 of the Software Definition Report (SDR) with the Software Baseline Documentation Number UCCSN-SDR-001. The results of the validation could be found in section 2 of the Software Implementation Report (SIR) with the Software Baseline Documentation Number UCCSN-SIR-001. Numerical results for the test are attached on a CD-ROM disk to the UCCSN-SIR-001 as appendix 1. Here is the short description of the test and numerical results

Test (Pure heat conduction in the square domain with constant heat flux boundary condition given on the wall)

The CHDHT v. 1.0 code does not have a capability of explicit modeling of the pure heat conduction problem but the pure heat conduction equation can be derived from the energy equation that CFDHT v.1.0 can solve. The pure heat conduction equation can be obtained in the code from the energy equation during the forced convection mode in case, velocities on the boundary are taken equal to zero when the forced convection type of heat transfer is activated through the input parameter file for the CFDHT v.1.0 software. As a result, the velocity values in the internal computational nodes will become equal to zero too. The energy equation becomes a simple heat conduction equation that has an analytical solution.

For the forced convection problem the dimensionless energy equation employed in the CFDHT v.1.0 has the form

$$\frac{\partial T}{\partial t} + u\frac{\partial T}{\partial x} + v\frac{\partial T}{\partial y} = \frac{1}{Pe}\left(\frac{\partial^2 T}{\partial x^2} + \frac{\partial^2 T}{\partial y^2}\right)$$

If the Peclet number is taken equal to $1 \cdot 10^{-5}$ by selecting the Prandtl number equal to 1.0 and the Reynolds number equal to $1 \cdot 10^{-5}$, then the diffusion terms will

dominate over the convection terms, and the latter terms could be neglected. Then the equation above can be reduced to a simple heat conduction equation

$$\frac{\partial T}{\partial t} = 1 \cdot 10^{5} \left(\frac{\partial^2 T}{\partial x^2} + \frac{\partial^2 T}{\partial y^2} \right)$$

The problem description is shown in the Figure below.

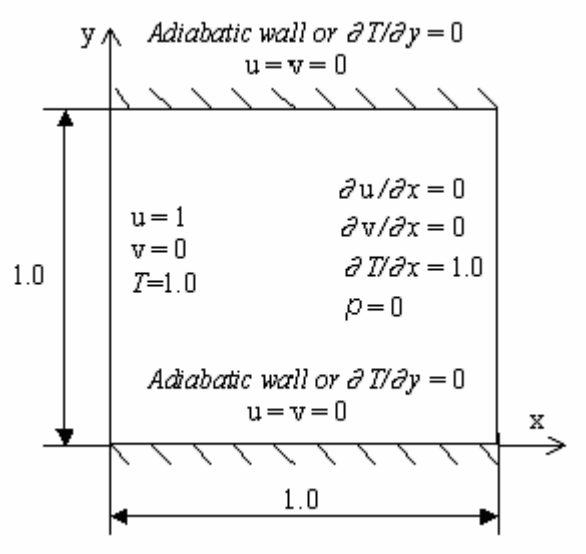

Figure 6-14 Computational domain with boundary conditions (UCCSN-SDR-001)

Here boundary conditions on the upper and lower walls are given as adiabatic or no flux boundary conditions, dimensionless temperature is equal to unity on the left boundary and dimensionless heat flux is equal to unity on the right boundary.

The analytical solution for this problem will be

$$T(x) = 1.0 + x$$

For acceptance, the difference between the analytical solution and the CFDHT v. 1.0 calculated temperatures shall be within 5 percent of the analytical results. This test case is a comparison with an analytical solution.

Results from the simulation are presented in Figure 1 for dimensionless static temperature.

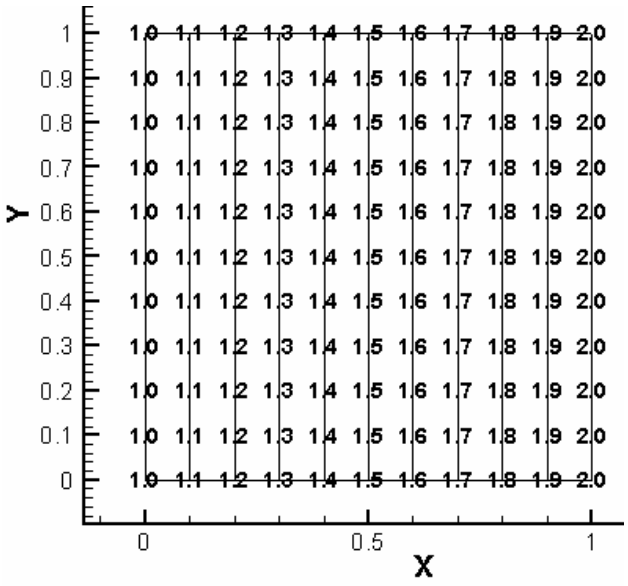

Figure 6-15. The square domain with isotherms and labels (UCCSN-SIR-001)

The acceptance criteria for this test case are based on CFDHT v. 1.0 results being within 0.05 of analytical values based on the solution $T(x) = 1 + x$, as established in Section 3.3.4 of the CFDHT v. 1.0 Software Definition Report. If the error between the results from CFDHT v. 1.0 and analytical values is within 5%, then the CFDHT model and the CFDHT v. 1.0 software passes that particular test.

This figure above shows that the CFDHT v. 1.0 results for the temperature at different distances from the left boundary meets the acceptance criteria as established in Section 3.3.4 of the CFDHT v. 1.0 Software Definition Report. The error in this case for different distances from the left boundary is 0%. Therefore, the CFDHT model as well as the CFDHT v. 1.0 software passes the acceptance criterion for this test case as defined in Section 3.3.4 of the CFDHT v. 1.0 Software Definition Report.

7 Conclusions

A new CFDHT model for thermal-fluid analyses of the Yucca Mountain drift for both pre-closure and post-closure periods has been developed. For the pre-closure period, the drift is considered isolated from the surrounding rock, and the only allowable path for heat removal from the drift is through the ventilating air. The 3-D analysis performed using STAR-CD v.3.150 for two speeds of the ventilating air, i.e. 1 m/s and 1.5 m/s showed that the speed 1 m/s is sufficient to reduce the temperature of the canister surface up to the value 154°C which is below the thermal goal of 350°*C* for the zirconium alloy cladding. However, to ensure a reliable reduction of temperature, the inlet speed of the ventilating air should be higher, and the speed 1.5 m/s results in better conditions for storing nuclear wastes during the pre-closure period with the maximum temperature on the canister surface being only 120°C. The maximum found temperature values in the domain are those on the last canister surfaces, i.e.154°C for the speed 1 m/s and 120°C for 1.5 m/s. However, since the computer model included just a part of the domain with 46 canisters instead of 67, the maximum temperature must be larger than 120°C for the speed 1.5 m/s and larger than 154°C for the speed 1 m/s. But the pattern of maximum temperatures is expected to remain similar so that the maximum temperature for both speeds is still expected to be on the last canister surface, and the temperature will not exceed 350°C, since the thermal loading of all canisters in the drift is considered identical. The found hot spots are behind the canisters downstream from the airflow.

For the pre-closure period, the thermal-fluid analyses of the drift are coupled with the calculation of heat conduction from the drift wall to the rock. The heat conduction problem solved using a 2-D finite-element code CFDHT v.1.0 provided the drift wall temperature boundary condition for the 3-D STAR-CD v.3.150 simulation of natural convection during the post-closure period. For the thermal loading of canisters equal to the thermal loading at the time of

emplacement, the found drift wall temperature was 140°C, the maximum temperature of the central canisters surface was 438°C which is above the thermal goal of 350°*C* for the zirconium alloy cladding. This high temperature is seemingly due to the fact that the value of the thermal loading of canisters used for calculations of natural convection in the post-closure period is somewhat higher than the actual thermal loading during the post-closure. The CFDHT model does not account for decaying the thermal loading with time. One more reason could be that, the CFDHT model does not account for the loss of heat from the canister surfaces by means of radiation, which is expected to be one of the major modes of heat transfer from the canister surfaces. The CFDHT model considers only the worst scenario in which the temperature on the canister surfaces at the described conditions will be 438°C.

The main potential sources of errors may include (1) Yucca Mountain site specific thermal and hydrothermal rock properties, (2) model configuration simplifications, (3) waste package/nuclear waste characteristics, (4) numerical discretization errors as well as iteration and successive approximation convergence errors. Within this complex system, the precision of overall model was objectively evaluated in section 6 of this report, independently from the input parameters and properties or the configuration of the model itself. Since the software STAR-CD v.3.150 and CFDHT v.1.0 were benchmarked using a set of verification test exercises, the precision of STAR-CD v.3.150 and CFDHT v.1.0 was maintained, therefore, the quality of the work specified in the current project was assured.

Uncertainty due to error propagation originated from all the factors described above, i.e. the input parameters, model configuration, simplifications, etc. is another major issue that is not routinely addressed in the current research and may lead to a separate research project using sensitivity analysis.

8 Inputs and References

1. Danko, G., Buscheck, T.A., Nitao, J.J. and Saterlie, S., "Analysis of Near-Field and Psychometric Waste Package Environment Using Ventilation," Proc. Intl. Conf. High Level Radioactive Waste Management, Las Vegas, Nevada, April 30–May 5, 1995, pp.323-330.

2. Akberov, R., Pepper, D.W., Chen, Y., Ponyavin V. and Hsieh, H., "Simulation of Convective Heat Transfer in the Yucca Mountain Repository," Proc. Intl. Conf. High Level Radioactive Waste Management, Las Vegas, Nevada, April 30–May 2, 2003, pp.661-666.

3. Moujaes, S. and Bhargava, A., "Simulation of Heat Transfer around a Canister Placed Horizontally in a Drift," Proc. Intl. Conf. High Level Radioactive Waste Management, Las Vegas, Nevada, May 22-26, 1994, pp.801-808.

4. Culbreth, W.G. and Pattisam, S., "Experimental Heat Transfer and Fluid Flow over Drift-Emplaced Canisters," Proc. Intl. Conf. High Level Radioactive Waste Management, Las Vegas, Nevada, May 22-26, 1994, pp. 772-779.

5. Launder, B.E. and Spalding, D.B., "Mathematical models of turbulence," London, Academic Press, 1972.

6. Baughn, J.W.; Hoflman, M.A.; Takahashi, R.K.; and Launder, B.E. 1984. "Local Heat Transfer Downstream of an Abrupt Expansion in a Circular Channel with Constant Wall Heat Flux", Journal of Heat Transfer, 106(4), 789-796. New York, New York: The American Society of Mechanical Engineers. TIC: 251949.

7. Kuehn, T.H. and Goldstein, R.J., "An Experimental and Theoretical Study of Natural Convection in the Annulus between Horizontal Concentric Cylinders," Journal of Fluid Mechanics, 74(4), 1976, pp.695-719.

8. Kuehn, T.H. and Goldstein R.J., "An Experimental Study of Natural Convection Heat Transfer in Concentric and Eccentric Horizontal Cylindrical Annuli," Journal of Heat Transfer (ASME), 100(4), 1978, pp. 635-640.

9. STAR-CD v. 3.150 Methodology, CD Adapco group, 2001.

10. CRWMS M&O 1999b Thermal Evaluation of Different Drift Diameter Sizes. BBA000000-01717-0210-00023 REV 00. Las Vegas, Nevada: CRWMS M&O. ACC: MOL.19981110.0001.

11. UCCSN-SDR-001.

12 UCCSN-SIR-001.

13 UCCSN-SDR-002.

14 UCCSN-SIR-002.

9 Attachments

There is no documentation for this report that cannot be included in the text.